SCIENTIFIC CULTURE
www.sci-cult.com

SCIENTIFIC CULTURE, Vol. 5, No. 2, (2019), pp. 7-20
Open Access. Online & Print

DOI: 10.5281/zenodo.2649499

MONITORING BUILDING MATERIALS EXPOSED TO MARINE ENVIRONMENT: EXAMPLES FROM FARASAN ISLANDS, SAUDI ARABIA

Abubakr Moussa

Department of Conservation, Faculty of Archaeology, Cairo University, 12611 Orman, Giza, Egypt

(dr_abubakr@msn.com)

Received: 29/09/2018
Accepted: 14/03/2019

ABSTRACT

This paper focuses on the role played by the marine environment conditions in the deterioration phenomena of building materials at the heritage houses in Farasan Islands, for this purpose bedrock and building materials from three ancient houses at two different islands in the red sea were studied comparatively; using XRD, SEM-EDS, Raman spectroscopy and XRF in order to identify their composition, and were investigated petrographically to determine the real response of the masonry structure to the deformation imposed at the surrounding conditions. Bedrock is mainly coral reef limestone and sandy limestone with high deposits of iron compounds and clay minerals, while building stone varies between coral reef limestone, dolomitic limestone and pure calcareous limestone, mortars and plasters also varies between lime and gypsum mortars. Foraminiferal shells are common in the studied stone samples. These building materials are widely affected by the surrounding marine climatic conditions including wind erosion and salt weathering.

KEYWORDS: Farasan islands; heritage houses; XRD analysis; SEM-EDS, Raman spectroscopy, XRF analysis, PM investigation; Building materials; Marine environment; Deterioration factors.

1. INTRODUCTION

Farasan archipelago (Fig. 1) is situated in the southern part of Red Sea (16° 20` -17° 20` N, 41° 24`-42° 26` E). It is far about 40 km from the Jizan coast (mainland) and attains a width of approximately 120 km in SE to NW direction. In this area, the Sea is very shallow (approximately100 meters in depth) and has a width of about 360 km between Jazan coast and the corresponding coast in Eritrea, the islands range in size from very small, a few m2, to the very large island of Farasan Al-Kabir about 381 km2 (Khalil, 2012, Al Mutairi and Al-Shami, 2014). These islands; would have been attached to the mainland at sea levels lower than about -20m, so that a human presence during the ancient era would not have depended on a technological capacity for sea travel. Generally; islands offer good marine conditions for the preservation and discovery of submerged landscape and archaeology; because they provide some protection from the full force of wave action associated with straighter and more exposed coastlines. The Farasan islands are composed of cemented coral platforms that have been variously uplifted and deformed by salt tectonics, resulting in a characteristically scalloped shoreline and a complex offshore topography including some very deep depressions (Abou Ouf and El. Shater, 1992, Bantan, 1999, Bailey et al., 2007a, Bailey et al., 2007b, 2012, 2014).

Figure 1. Location map of Farasan islands

The studied heritage houses from Farasan islands are: The Hussein Al-Refaie house: 1912, the Ahmed Al-Refaie house: 1922, and The house of German: 1901 (Fig. 2); the first two houses were built by pearl merchants carrying the same names, the houses are located in the biggest one of Farasan islands which named "Farasan Al-Kabir". Architecturally the two houses are following the ottoman style, with some richness in decorations, ornaments are carried out using imported raw materials; as the local environment is very poor towards wood and masonry. The third house "German house" or "Germal house" according to the local dialect; is located in Qummah island which is about 8km from Farasan Al-Kabir, this house was built in 1901 as a coal store to be used by the German forces, but due to political issues between Germany and Turkey; the project was uncompleted. The present study aims essentially to assess which numerous causative factors play roles of degradation and deterioration situation in each element of the Farasan heritage houses. The study also makes it possible to know the used research methodology including the identification of building materials and the damage situation at Farasan islands using the direct observation and primitive monitoring evaluation.

Figure 2. A: The house of German. B: Ahmed Al-Refaie house. C: Hussein Al-Refaie house

2. SAMPLING AND METHODOLOGY

Bedrock samples derived from the shores of Farasan islands were studied by mean of X-ray diffraction (XRD) using a Bruker's X-ray powder diffractometer (D8 Advance, Cu Kα, λ = 0.154 nm), and Raman scattering spectra which were recorded on a LABRAM-HR Raman spectrometer excited with a 514.5 nm Ar + laser, moreover, mass contents were measured by thermal gravimetric analysis (SDT Q600), field-emission scanning electron microscopy (SUPRA 40 ZEISS, Germany, SEM-EDS). Chemical composition and petrographic properties of the building materials at Farasan heritage houses including stone, mortars and plasters were studied to identify their characteristics. X-ray diffraction (XRD) analysis was performed using a Philips (PW1840) diffractometer with Ni-filtered Cu-Kα radiation. The samples were scanned over the 5-70° 2θ intervals at a scanning speed of 1.2° min-1. A° quantitative estimate of the abundance of the mineral phases was derived from the XRD data using the intensity of certain reflections and external standard mixtures of minerals compared to the JCPDS standards of 1967. The chemical analysis of some samples from the building materials was carried out using X-ray fluorescence (Axios spectrometer, PANalytical Company, Netherlands). The prepared thin-sections (thickness 30 µm) were examined in the crossed-polarized light (XPL) by a Nikon Eclipse E600 microscope with

photographic attachments include PixeLINK PL-A623 digital camera.

3. CLIMATIC CONDITIONS

Based on the data obtained from the Saudi meteorological agency and climate experts; in addition to the data obtained from the specialized websites, it is concluded that precipitation on Farasan islands is very rare in, the minor amount of rainfall ranges between zero and 2 mm per month, this can be registered in most months of the year while the maximum precipitation amount ranges from 5 to 10 mm per month, the rainy months are four: June, July, August and September, some seasonal rains can cause floods (Fig.3).

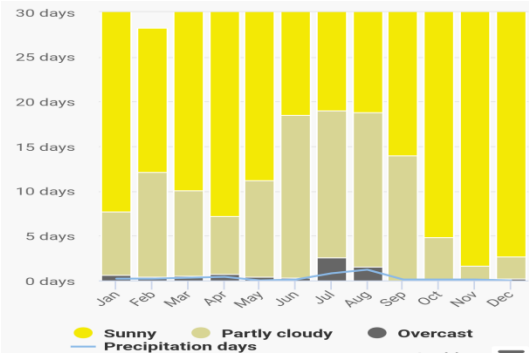

Figure 3. Climate graph shows the cloudy, sunny and precipitation days upon Farasan Islands (www.meteoblue.com)

The combined effect of wind and precipitation determines the specific forms of wetting, washing out or the dangerous impact of hail on exposed surfaces, the primary source of humidity and salts on external walls especially in islands are wind and sea spray, south western wind on Farasan islands is the dominant, it blows for approximately 1300 hours per year with a speed average from 5 to 12 km per hour (Fig. 4).

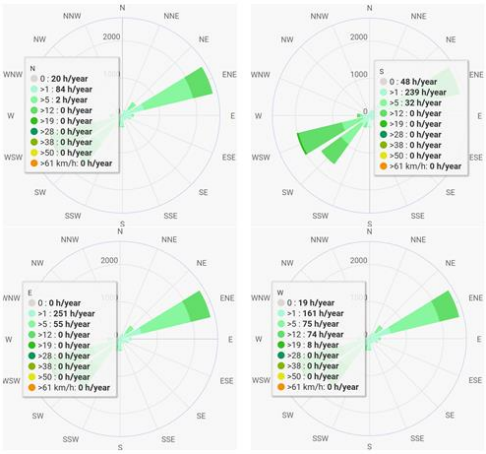

Figure 4. Wind roses showing the direction and speed of wind on Farasan Islands (www.meteoblue.com)

Concerning heat; Farasan islands are registering high temperature year-round, temperature is often around 30 °C and 35 °C, but it goes higher than 40 °C in summer months (Fig. 5).

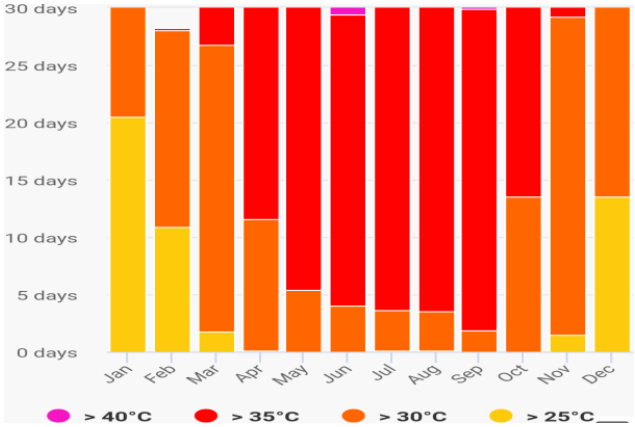

Figure 5. Climate graph shows the average temperature upon Farasan Islands (www.meteoblue.com)

4. RESULTS

4.1. Bedrock results

The SEM investigation of the first bedrock sample has shown that the sample is a coarse grained rock with high deposits of salt crystals, cohesion between crystals is lost in some places, while the fabric of the sample seems to be affected badly by act of weathering, the texture of the sample is not typical all-over the scanned areas (Fig. 6). The second bedrock sample has shown more salt deposits but harder appearance of fabric and texture, weathered shape is the common factor between the three samples (Fig. 7). The third sample represents the typical shape of the limestone derived from the coral reefs surrounding Farasan islands, marine weathering and deposited salts is very clear upon the scanned surface (Fig. 8).

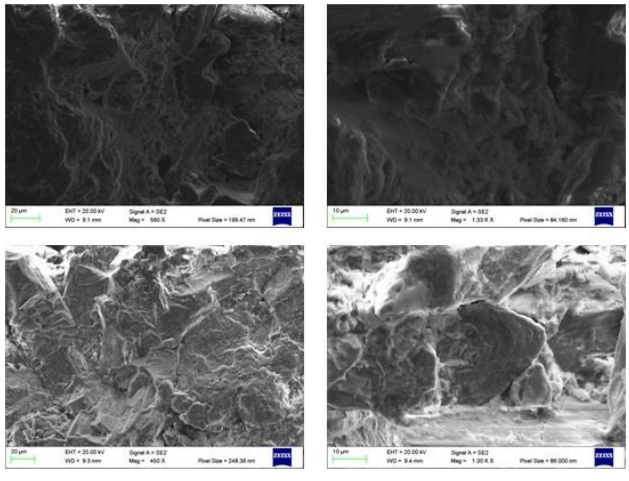

Figure 6. Scanning electron micrographs of the first bedrock sample from Farasan islands

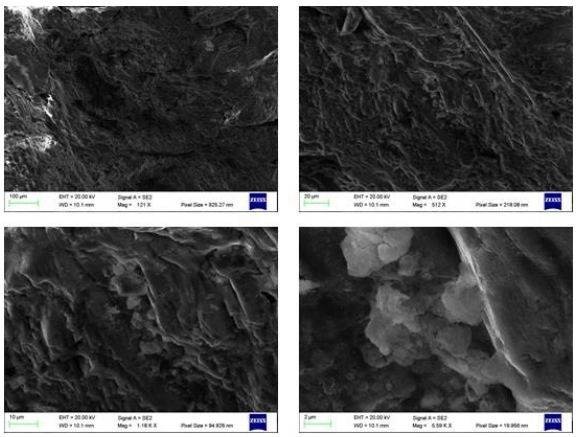

Figure 7. Scanning electron micrographs of the second bedrock sample from Farasan islands

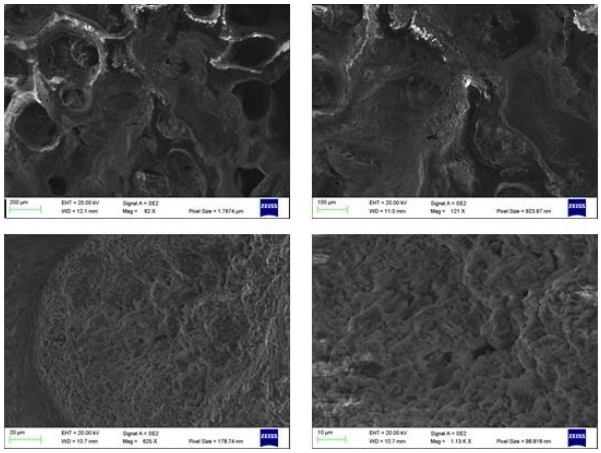

Figure 8. Scanning electron micrographs of the third bedrock sample from Farasan islands

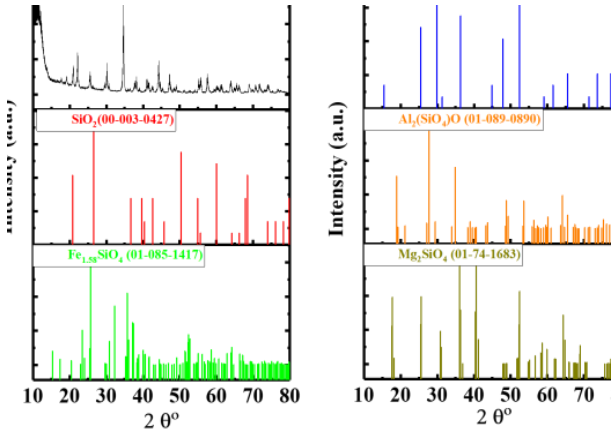

Figure 9. XRD pattern of the first bedrock sample from Farasan islands

According to the XRD analysis of the three bedrock samples; the first bedrock sample composes mainly of sandy clays with high ration of magnesium silicate, the sample contains a significant ration of quartz, aluminium silicate and iron silicates (Fig. 9), the second bedrock sample has shown approximately the same components of the first one, moreover; halite appears to be one of the major compounds in its matrix (Fig. 10), while the third bedrock sample is mainly calcite with halite and quartz, iron compounds were also detected abreast with aluminium and magnesium compounds (Fig. 11)

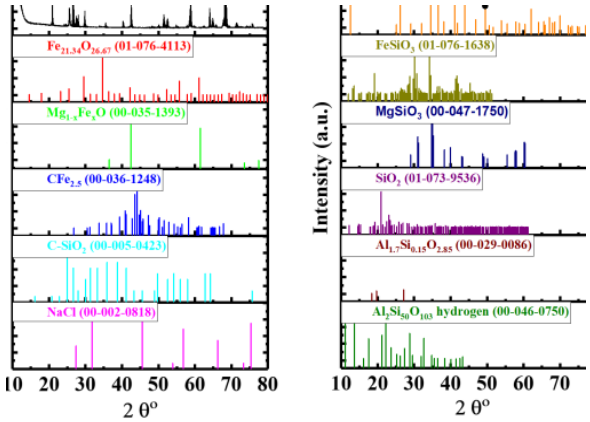

Figure 10. XRD pattern of the second bedrock sample from Farasan islands

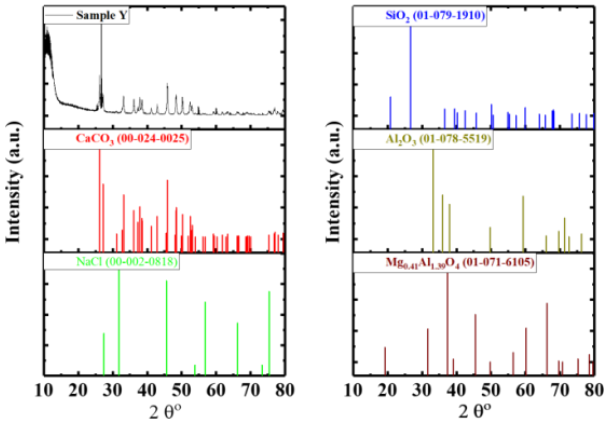

Figure 11. XRD pattern of the second bedrock sample from Farasan islands

XRD results were emphasized by mean of SEM-EDS, the first sample composes of about 57% oxygen, 15% carbon, 8% aluminium, 6% silicon, 5% iron, 3% sodium, 3% magnesium and about 3% of chlorine (Fig. 12), the elemental mapping (colour and distribution of the elements inside the sample) is represented in Fig. 13.

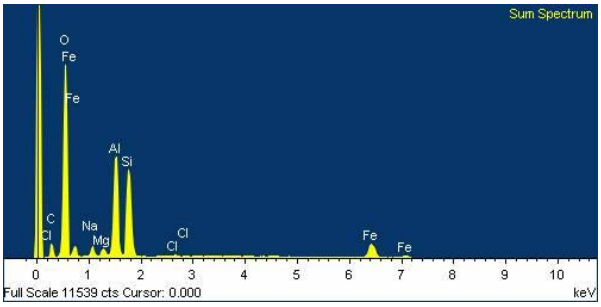

Figure 12. SEM-EDS spectra of the first bedrock sample from Farasan islands

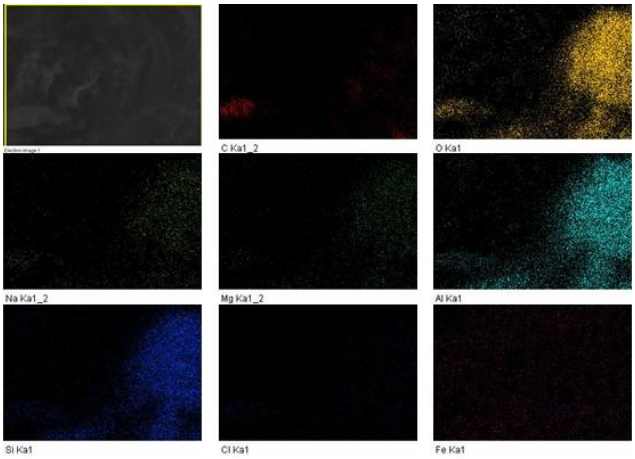

Figure 13. SEM-EDS elemental mapping of the first bedrock sample from Farasan islands

The second bedrock sample composes of about 40% oxygen, 20% carbon, 12% silicon, 10% sodium, 8% calcium, 4% iron, 4% chlorine, 1% sulphur and 1% potassium (Fig. 14); the elemental mapping is represented in Fig. 15.

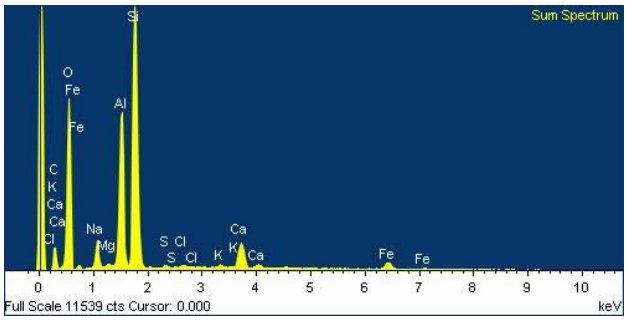

Figure 14. SEM-EDS spectra of the second bedrock sample from Farasan islands

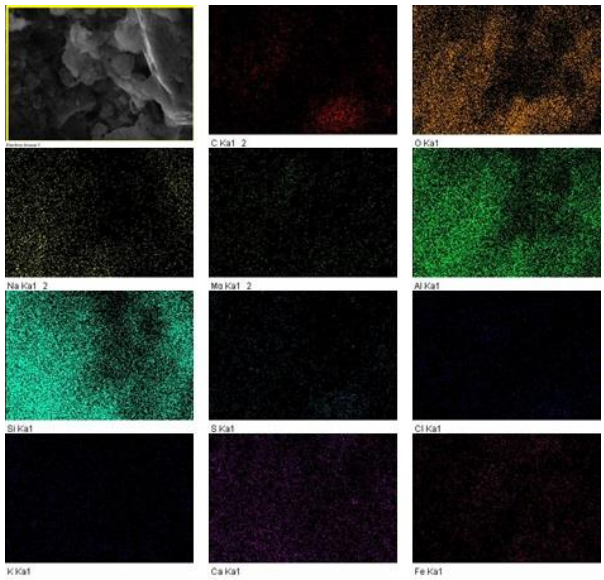

Figure 15. SEM-EDS elemental mapping of the second bedrock sample from Farasan islands

The EDS analysis has revealed oxygen as the dominant component in the third bedrock sample with 45% ratio, in addition to 31% calcium, 14% carbon, 3% sodium, 3% magnesium, 2% silicon, 1% aluminium and 1% sulphur (Fig. 16), the elemental mapping (colour and distribution of the elements inside the sample) is represented in Fig. 17.

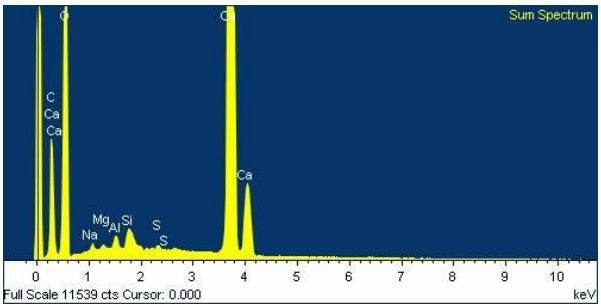

Figure 16. SEM-EDS elemental mapping of the second bedrock sample from Farasan islands

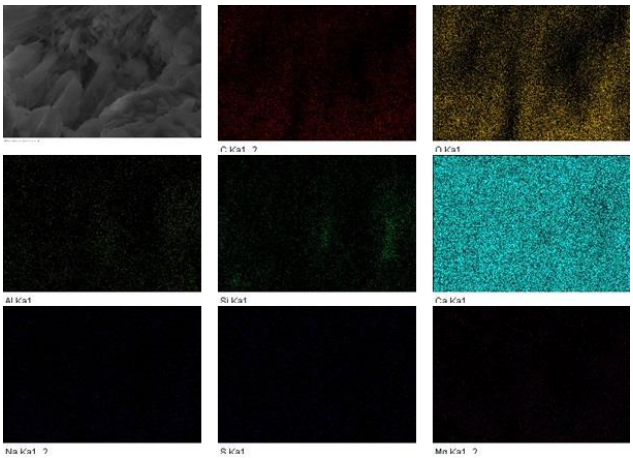

Figure 17. SEM-EDS elemental mapping of the second bedrock sample from Farasan islands

Further analysis for the bedrock samples has been carried out by mean of Raman spectroscopy; the first sample has shown the wavenumbers of C-C bands at 200-400 cm^{-1} and at 630-1250 cm^{-1}, the sample also shows Xmetal-O band at 150-430 cm^{-1}, while Si-O-Si, Si-O-C, and C=S bands appeared in the samples at 1020-1225 cm^{-1}, and OH bands appeared at 2880-3530 cm^{-1} (Fig. 18).

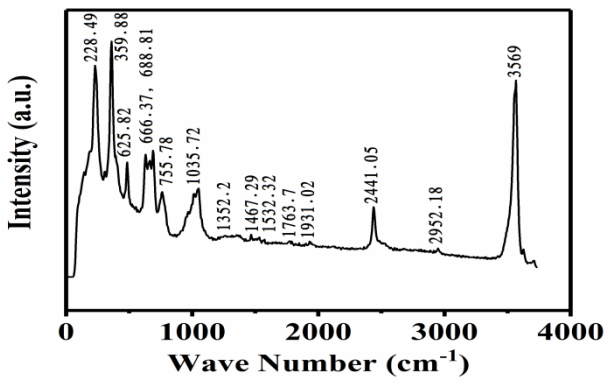

Figure 18. Raman spectrum of the first bedrock sample from Farasan islands

Second sample has shown the wavenumbers of Xmetal-O bands at 150-430 cm^{-1}, Si-O-Si bands at 460-550 cm^{-1}, wavenumber of anhydrite band at 1740-1830 cm^{-1}, thiol band at 2530-2610 cm^{-1}, and OH band at 2880-3530 cm^{-1} (Fig. 19).

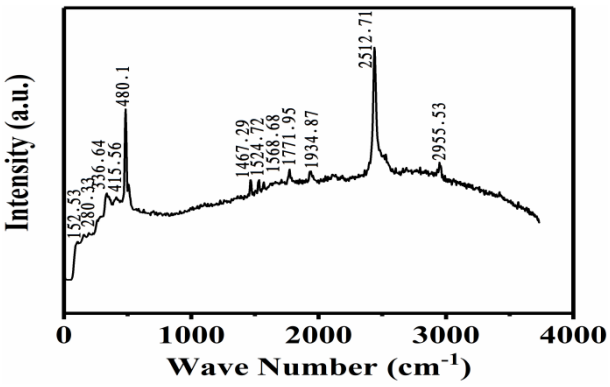

Figure 19. Raman spectrum of the second bedrock sample from Farasan islands

Third sample has shown the wavenumbers of Xmetal-O bands at 150-430 cm^{-1}, Si-O-Si and Si-O-C bands at 1010-1095 cm^{-1}, C=C band at 1625-1680 cm^{-1}, anhydrite band at 1740-1830 cm^{-1}, thiol band at 2530-2610 cm^{-1}, and OH band at 2880-3530 cm^{-1} (Fig. 20).

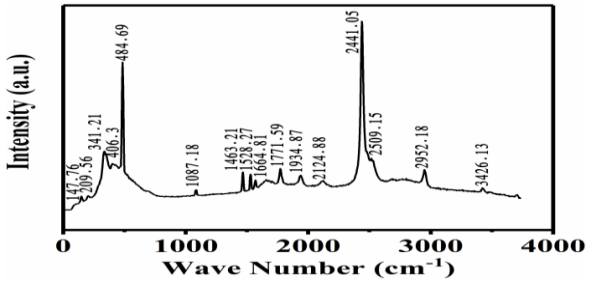

Figure 20. Raman spectrum of the third bedrock sample from Farasan islands

4.2. German house XRD results

Four limestone samples were analysed in order to differentiate between them, based on the XRD analyses; the first limestone sample which was taken from the inner side of the building walls; composes of 54.4% calcite and 45.6% aragonite (Fig. 21). Second limestone sample was derived from the outer face of the walls which is exposed to weathering factors; the XRD analyses proved that the sample composes of 80.1% calcite and 19.9% dolomite (figure 22). Third limestone sample was derived from the weathered internal columns of the building; the sample contains 70.1% aragonite, 19.1% calcite and 10.1% halite (Fig. 23). Fourth limestone sample was derived from the lintels of the building; the sample composes of 58.7% calcite, 37.8% dolomite and 3.5% halite (figure 24). Concerning mortars; two mortar samples were analysed from the building: the first was derived from the walls and composes of 59.5% calcite, 33.3% aragonite and 7.2% dolomite (Fig. 25), while the second mortar sample was derived from the remains of the internal columns and composes of 56% calcite, 36.4% halite and 7.6% quartz (figure 26). Plaster which is used to protect masonry elements from weathering factors and providing a paintable surface was analysed, outer and inner plaster in the building have the same composition which is 100% calcite according to the XRD analyses of two plaster samples (figures 27&28). As for weathering products; two samples were investigated, the first one is a hard crust sample from the outer facades of the building and it composes of 78.9% calcite and 21.1% dolomite (Fig. 29), the second sample is derived from the inner columns and it composes of 57.4% calcite, 38.8% aragonite, 2.2% quartz and 1.6% halite (figure 30).

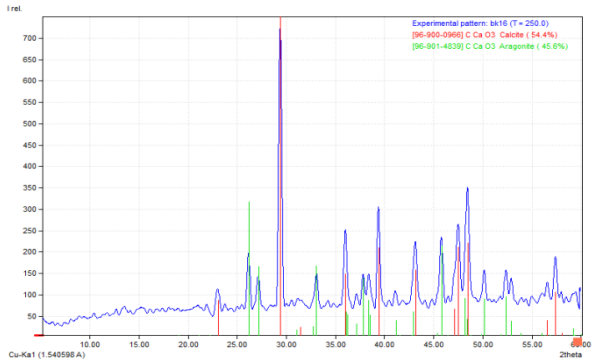

Figure 21. XRD pattern of the first limestone sample from the house of German

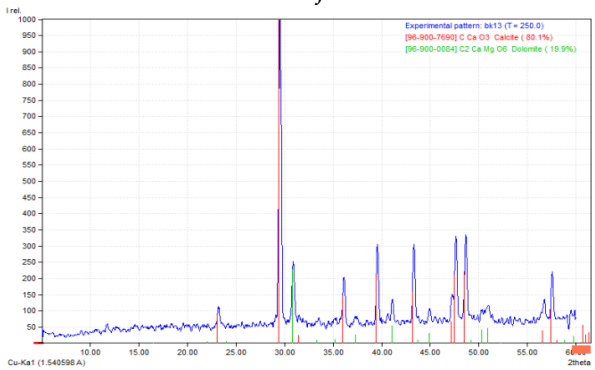

Figure 22. XRD pattern of the second limestone sample from the house of German

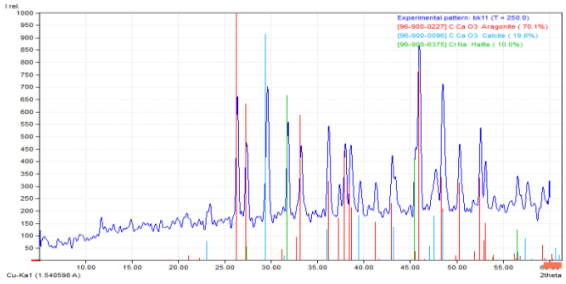

Figure 23. XRD pattern of the third limestone sample from the house of German

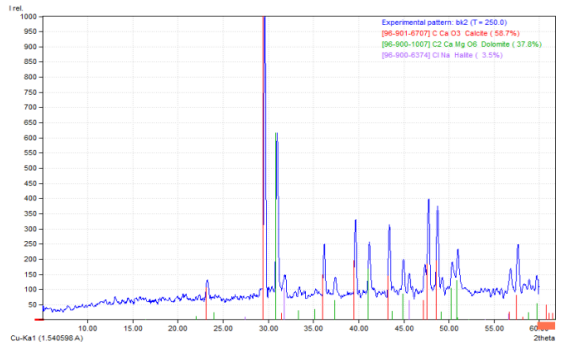

Figure 24. XRD pattern of the fourth limestone sample from the house of German

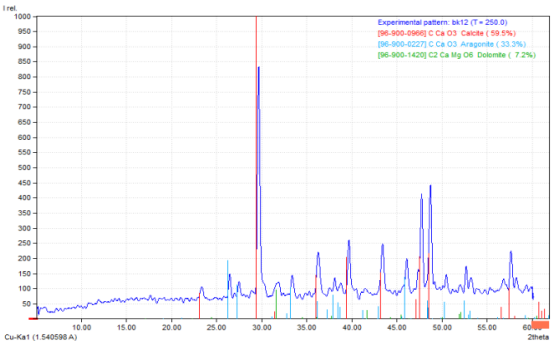

Figure 25. XRD pattern of the first mortar sample from the house of German

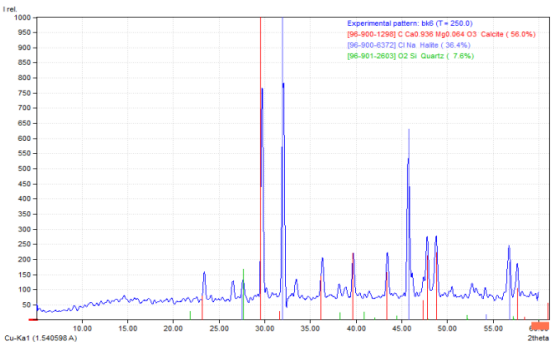

Figure 26. XRD pattern of the second mortar sample from the house of German

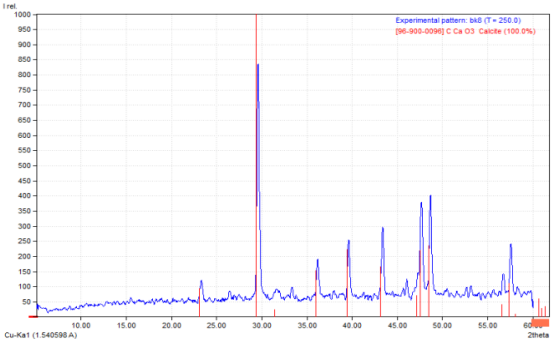

Figure 27. XRD pattern of the first plaster sample from the house of German

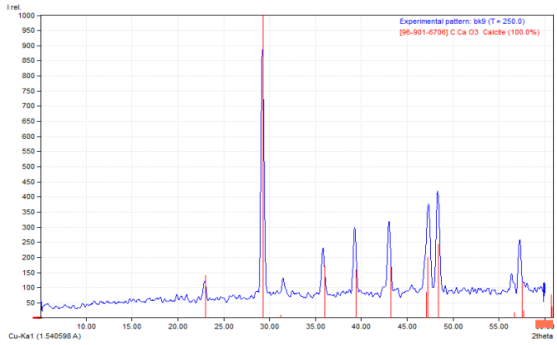

Figure 28. XRD pattern of the second plaster sample from the house of German

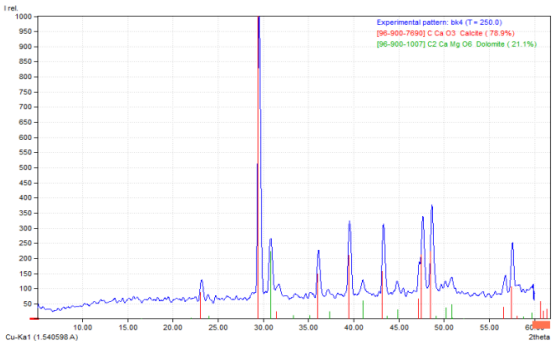

Figure 29. XRD pattern of the first weathered sample from the house of German

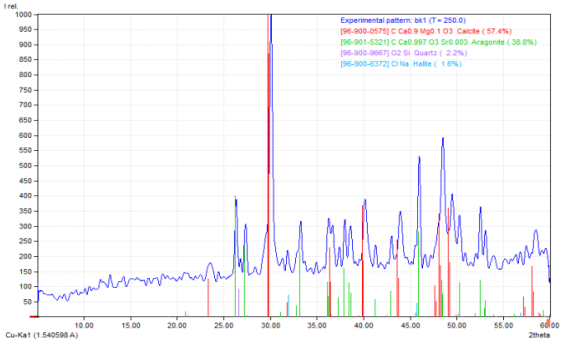

Figure 30. XRD pattern of the second weathered sample from the house of German

4.3. Ahmed Al-Refaie house XRD results

Two stone samples were analysed from this house; the first one composes of 64.1% calcite and 35.9% aragonite (Fig. 31), while the second one composes of 100% calcite (figure 32). Based on the XRD results; mortar in the studied house composes of 70.8% gypsum and 29.2% anhydrite (figure 33), while plaster composes of 74.2% gypsum and 25.8% anhydrite (figure 34), white wash is lime and composes of 67.1% calcite and 32.9% dolomite, (Fig. 35), concerning ornaments and decorations; it was found that gypsum was the used raw material and the analysed sample composes of 84.6% anhydrite and 15.4% gypsum (Fig. 36).

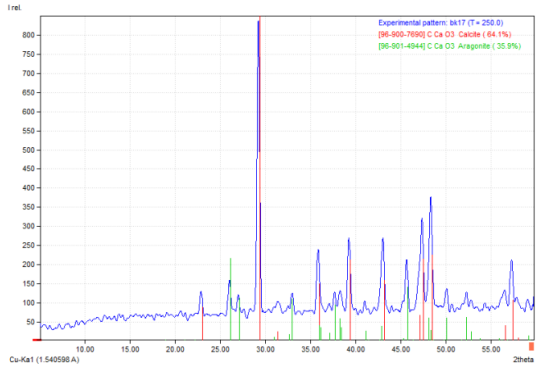

Figure 31. XRD pattern of the first limestone sample from Ahmed Al-Refaie house

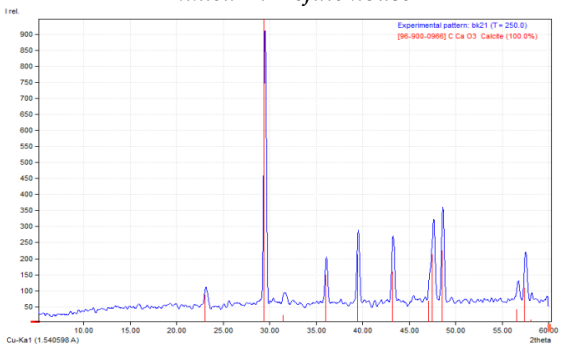

Figure 32. XRD pattern of the second limestone sample from Ahmed Al-Refaie house

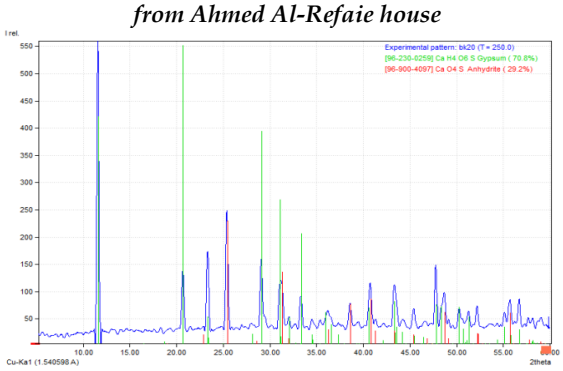

Figure 33. XRD pattern of the mortar sample from Ahmed Al-Refaie house

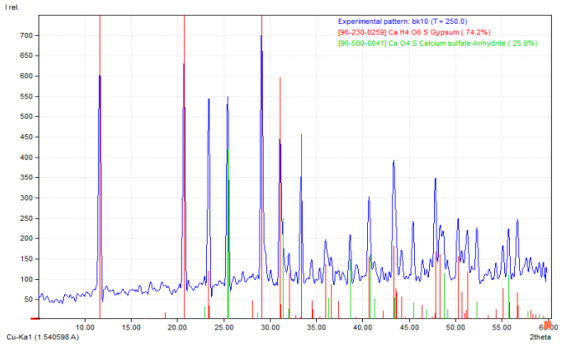

Figure 34. XRD pattern of the plaster sample from Ahmed Al-Refaie house

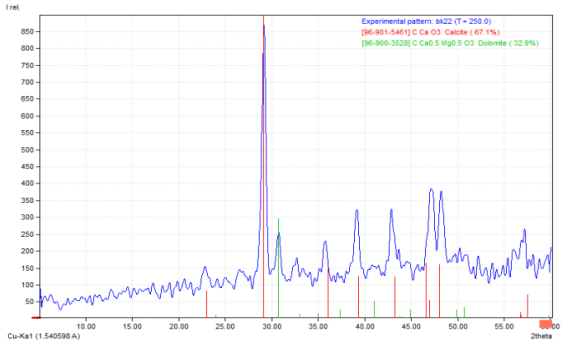

Figure 35. XRD pattern of the whitewash sample from Ahmed Al-Refaie house

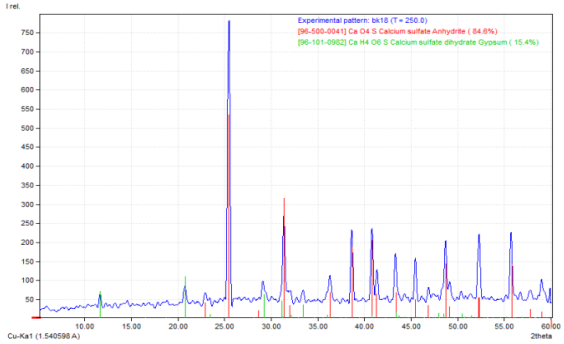

Figure 36. XRD pattern of the ornament sample from Ahmed Al-Refaie house

4.4. Hussein Al-Refaie house XRD results

According to XRD analysis; building stone in this house is a fine limestone composes of 100% calcite (Fig. 37), while mortar is pure gypsum composes of 100% calcium sulphate dihydrate (Fig. 38), plaster sample from the house composes of 88.4% gypsum and 11.6% anhydrite (Fig. 39), white wash in this house composes of 89.3% calcite and 10.7% dolomite (Fig. 40), two samples from the ornaments and decorations in this house were analysed; the first one composes of 73.7% gypsum and 26.3% anhydrite (figure 41), while the second one composes of 100% gypsum (Fig. 42).

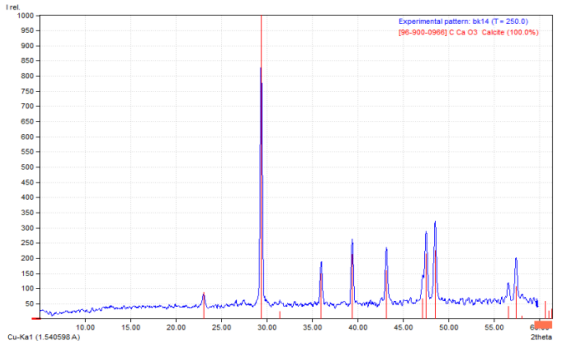

Figure 37. XRD pattern of the limestone sample from Hussein Al-Refaie house

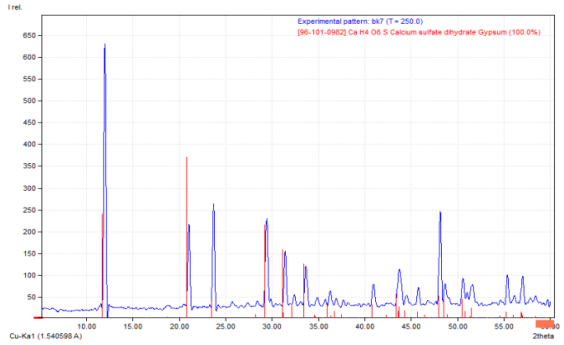

Figure 38. XRD pattern of the mortar sample from Hussein Al-Refaie house

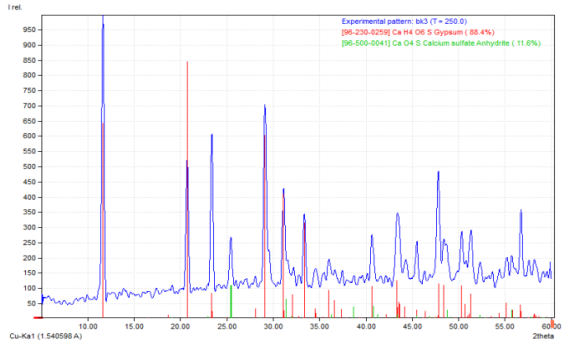

Figure 39. XRD pattern of the plaster sample from Hussein Al-Refaie house

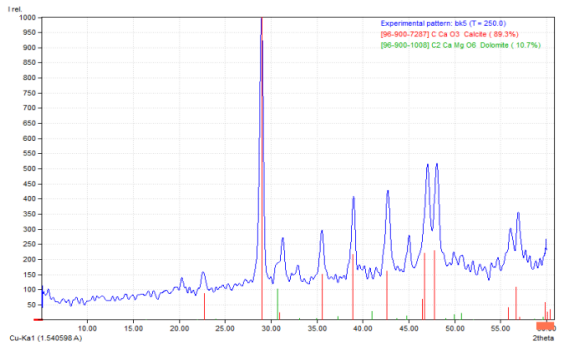

Figure 40. XRD pattern of the whitewash sample from Hussein Al-Refaie house

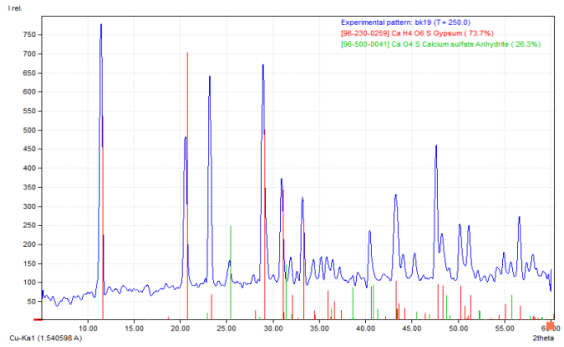

Figure 41. XRD pattern of the first ornament sample from Hussein Al-Refaie house

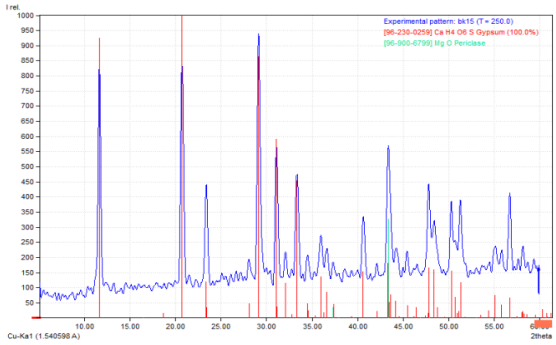

Figure 42. XRD pattern of the second ornament sample from Hussein Al-Refaie house

5. X-RAY FLORESCENCE ANALYSES

Six samples were analysed by mean of XRF, tow samples from each house; the first sample is a plaster sample from the house of German, calcium, sulphur, silicon and magnesium are the dominant components of the sample with traces of iron, sodium and chlorine, the sample contains 20% loss on ignition ratio, the second sample is mortar sample from the same house, calcium, sulphur, silicon, magnesium, iron and chlorine are the main components, while sodium, and potassium are found as traces, the sample contains 23% loss on ignition ratio. The third sample is a limestone sample from Ahmed Al-Refaie house, its main components are calcium, silicon and aluminium, chlorine and sodium were detected as traces, the sample contains 42.5% loss on ignition ratio, the fourth sample is a mortar sample from the same house, it contains calcium, sulphur and silicon as major, while chlorine, sodium and iron are found as minor, the sample contains 27.80% loss on ignition ratio. Fifth sample was taken from the outer plaster of Hussein Al-Refaie house, calcium, sulphur and silicon with other traces are its components in addition to 22% loss on ignition ratio, the last sample is derived from the ornaments at the same house, calcium, sulphur and silicon were detected with other minor components as shown in Table (1), the sample contains 27.50% loss on ignition ratio.

Table 1: The chemical composition of the samples studied by mean of XRF

	1	2	3	4	5	6
CaO	61.58	53.80	47.80	35.50	32.50	34.90
SO_3	9.13	13.40	0.52	29.80	39.88	30.40
SiO_2	3.00	3.18	4.70	2.35	2.74	3.34
MgO	2.18	1.78	0.94	0.87	0.70	0.62
Fe_2O_3	0.94	1.14	0.72	0.81	0.50	0.71
Al_2O_3	0.72	0.94	1.35	0.54	0.73	0.74
SrO	0.68	0.73	0.07	0.60	0.59	0.72
Na_2O	0.49	0.58	0.45	0.38	-	0.33
K_2O	0.23	0.27	0.21	0.35	0.13	0.18
P_2O_5	0.17	0.11	0.07	0.04	0.04	0.04
NiO	0.03	-	-	-	-	-
Cl-	0.83	1.00	0.46	0.83	0.10	0.27
Br	-	0.02	-	-	-	-

Mn	-	-	-	-	-	0.05
TiO	-	-	0.18	0.11	0.06	0.09
Cr_2O_3	-	-	-	-	-	0.10
LOI	20.00	23.00	42.50	27.80	22.00	27.50
Total	99.98	99.95	99.96	99.98	99.98	99.99

6. PETROGRAPHIC INVESTIGATION

6.1. German house petrographic results

Petrographic examinations of ancient stones allow us to determine specific minerals and rock textures, coarseness, and the relative or quantitative percentage of various constituents (Reedy, 1994). The petrographic and chemical study of the mortars gives information on the stone used to make it, on the technology used in the manufacturing phases (presence of lumps, charcoal, additives, etc.) and in the burning (Pecchioni et al., 2006). Petrographically, four samples from the German house were studied. The first and second samples were derived from the limestone blocks exposed to weathering. Wackestone is the most common type consisting the limestone blocks of the German house; both samples contain a ground mass of micrite (chalky limestone); the first contains fragments of algae, while the second sample contains fragments of shells (foraminiferal shells). Third sample was derived from the internal side of the walls, the sample is fossiliferous biomicrite or dolomitic skeletal packstone, and it contains brownish glauconite and nimolites. The fourth sample is a mortar sample; the petrographic analysis of the sample showed some common characteristics of mortars with respect to the matrix, which is mainly composed of lime with different types of aggregates. The main aggregate used in the mortars was sand, it can be also observed that the mortar is made of pure lime, originated from burning-slaking process, limestone (dolomite) pebbles and fragments are clearly visible together with few sub-rounded and rounded quartz grains of variable dimensions, fragments of algae, some shell fragments of gastropods and foraminifera were detected. The microphotographs of the petrographic examinations carried out on thin-sections prepared on stone and mortar samples are given in Fig.43 to Fig.46 inclusive.

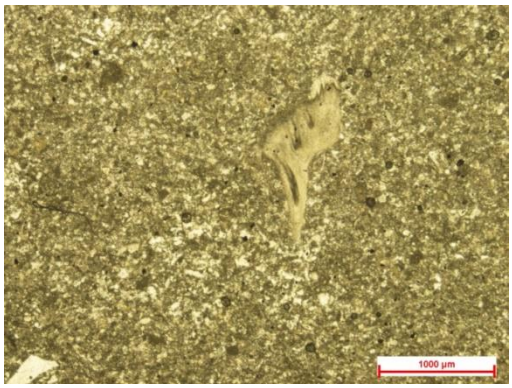

Figure 43. Photomicrograph of the first limestone sample from the house of German

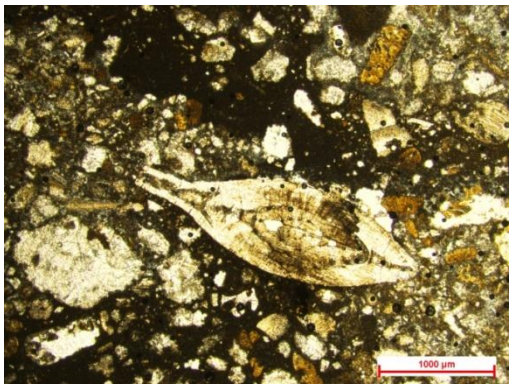

Figure 44. Photomicrograph of the second limestone sample from the house of German

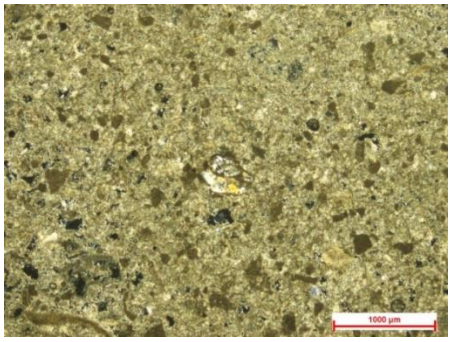

Figure 45. Photomicrograph of the third limestone sample from the house of German

Figures 46. Photomicrograph of the studied mortar sample from the house of German

6.2. Ahmed Al-Refaie house petrographic results

Petrographically; limestone in this house is algal limestone or skeletal packstone containing pellets of chalk and algal biomicrite, the skeletal particles are mainly represented by benthonic and minor planktonic foraminiferal tests in addition to some algal fragments (Fig. 47), the result of the XRD analysis (Figs 12&13) supports the mineral composition of the rock that revealed from the thin section investigation. Concerning mortar (figure 48); the investigation showed very few fine quartz grains, traces of gypsum particles and dolomite rhombs could be observed in some parts of the sample. Some additives of crushed igneous volcanic rocks (mainly basaltic rocks) are observed in the sample; these volcanic rocks are common in the red sea islands and are covered sometimes with coral reefs. It can be said that these dark coloured additives of feldspars phenocrystals are trial for giving some hydraulic properties into the mortar "a local trial for volcanic ash or pozzolanic additives".

Figures 47. Photomicrograph of the studied limestone sample from Ahmed Al-Refaie house

Figures 48. Photomicrograph of the studied mortar sample from Ahmed Al-Refaie house

6.3. Hussein Al-Refaie house petrographic results

Petrographically; limestone in this house (Fig. 49) is a sandy limestone containing some intraclasts of carbonate rock fragments or feldspathic rock fragments, and pelecyponda shell fragments imbedded in dolomitic micrite which partially recrystallized into microsparry calcite. The stone has numerous pores, shrinkage microcracks and microvoids. Some voids are shown with partially filling of zoned idiotopic ferron dolomite or ankerite rhombs. Mortar sample has shown the same results previously shown in Ahmed Al-Refaie house mortar sample in addition to over growth of calcium carbonate crystals, which means that there are voids in the matrix or there was a precipitation from a dissolved calcium carbonate, the sample showed also some oolitic fossils (Fig. 50).

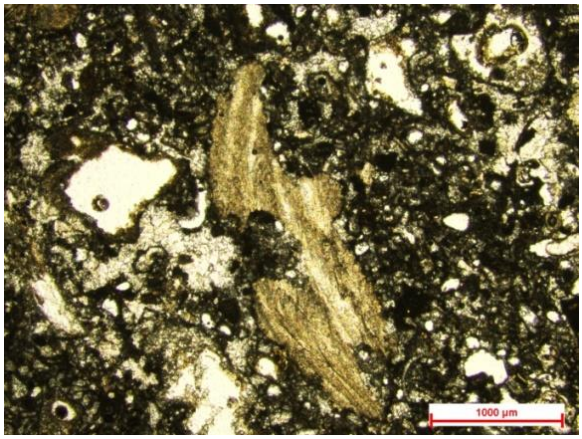

Figures 49. Photomicrograph of the studied limestone sample from Hussein Al-Refaie house

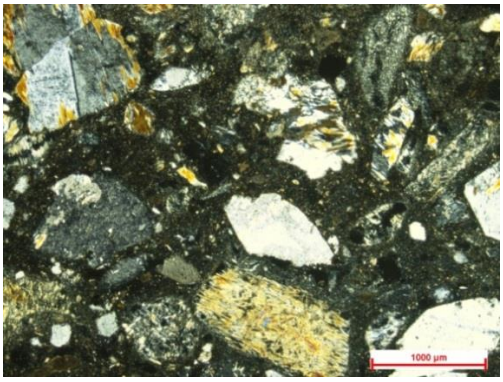

Figures 50. Photomicrograph of the studied mortar sample from Hussein Al-Refaie house

7. DISCUSSION

Geologically; whole-sediment mineralogy of the Jazan shelf is characterized by the presence of carbonates, quartz and feldspars, carbonates are mainly represented by aragonite and high Mg-calcite (Abou Ouf and El Shater, 1992). Concerning climate; tem-

perature on the islands ranges from 21.9 °C minimum in January to 37.7 °C maximum in July (Bantan, 1999), the surface water temperature ranges between 25.5 °C in winter and 33 °C in summer, while the surface water salinity ranges from 37.5% in winter and 39% in summer (Ouf and El Shater, 1992). Wind represents an erosion factor, its effect abreast with sea spray may lead to total loss of building materials, coral reef building limestone in Farasan islands has transformed into a spongy texture by the act of wind. Unlike previous studies; the current study defines iron oxides (mainly hematite) in both bedrock samples and building stone samples, the latter has shown a significant quantity of iron when analysed by mean of XRF, moreover; iron oxides were detected in both mortars and plaster layers in the three studied houses, the field investigation at Farasan islands made it clear that iron corrosion-like spots are very clear upon building stones and mother rocks all-over the area (Fig. 51).

XRD, SEM-EDS and Raman spectroscopy of the bedrock samples made it clear that clay minerals, quartz and dolomite are contained in the mother rock, this represents more weakness and erodibility to the already degradable building materials derived from this bedrock, moreover; the chemical analysis by mean of XRF has shown that the loss on ignition ratio varies from 22% to 42.5%, what makes this amount such high is the nature of building materials which have a significant amount of organic substrates (shells and fossils) in their physical composition, the maximum loss on ignition ratio was registered for coral reef building limestone, which acts a abuilding material and as a source for other building materials, this loss stands basically for the organic materials found in the sample, or for the amount of calcium carbonate burnt during firing process of the sample, field investigation emphasises that the nature of building materials is the main deterioration factor affecting Farasan heritage houses (figure 52).

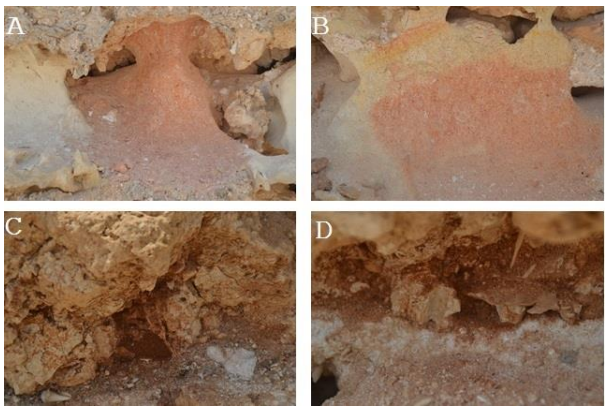

Figures 51. Four different shots from Farasan islands showing the presence of iron oxides in both building stones of the house of German (A,B) and bedrock of Farasan Alkabir (C,D)

Figures 52. Four different shots from Farasan islands (German house) showing the effect of wind on building stones (A), the typical shape of coral building limestone (B,C) and the high amount of shells and fossils in plaster layer (D)

According to XRD analyses and petrographic investigation; the building limestone in the studied houses is derived from the local rocks in the islands, as it contains the dominant components (calcite, aragonite, dolomite and halite) of the geological members, some samples showed building stone as pure calcite, that may refer to high experience of rock-cut process, or this casing stone has been imported to the islands. Khalil (2012) referred to white limestone as a geological member under the coral reef limestone of the Farasan formation, this member varies in thickness between 5m to 15m. Mortars and plasters at the house of German have almost the same composition and the same shape of the stone, which emphasizes that these mortars and plasters were prepared from local rocks; calcite is their dominant component abreast with aragonite and dolomite. Both calcium and Magnesian limes are suitable for building purposes and, historically, chosen depending on local geology (English Heritage Directory, p.6), but when the slaking process of lime is not intense enough, the final product could contain some crystalline CaO and MgO, The hydration reactions of MgO and CaO are slow and expansive and they can cause cracking problems and even the breakdown of mortars (Palomo et al., 2004). Dolomitic lime can perform well in mortar stabilization, although the magnesium fraction reacts more slowly than the calcium fraction (Lime-treated soil construction manual 2004). Mortars in the two other houses have the same composition; gypsum is the dominant compound with minor percentage of anhydrite. Middle Miocene sedimentations are located on the north of the Farasan Island, and represented by anhydrite, gypsum and halite deposits (Khalil, 2012),

thus it cannot be said safely that anhydrite here is a result to the dehydration of gypsum. In sea water; gypsum precipitates out first, followed by anhydrite deposits, the latter may remain as such for over millennia, however in the presence of groundwater it can turn into gypsum to some 15 to 40 meters depth (Charola et al., 2007). Previous authors state that the dehydration of gypsum to hemihydrate does not occur on monuments (Charola and Centeno 2002). This does not preclude that gypsum, particularly in cryptocrystalline forms, may partially dehydrate and eventually rehydrate giving rise to further contraction–expansion cycles (Charola 2003). This hypothesis is supported by the detection of both anhydrite and gypsum in some of the studied samples from Farasan islands. Halite salts were detected in many samples with high ratio; halite in solution is mobile and able to break up many crystalline structures when it re-crystallizes. It is capable of retaining the adsorbed humidity in the masonry, most salts, including chlorides and sulphates, have high coefficients of volumetric expansion and show a volume increase with higher temperature, rainwater dissolves halite first, then gypsum, anhydrite (Wüst et al. 2000), that means voids and gabs inside and on the surface of building materials. The studied white wash samples are pure lime; this is an indicator for fresco technique wall painting, however no pictorial layer found. Petrographically; Farasan islands are characterized by muddy sand, seagrasses, and green filamentous algae, the islands have sandy substrates with indications of shoreward transport in addition to dissolution, bioerosion in the calm waters, abrasion, and breakage in the nearshore sediments (Abu-Zied et al., 2011).

8. CONCLUSIONS

This study proves that building materials at the heritage houses in Farasan islands are suffering serious deterioration factors including wind erosion, salt weathering, variation of air temperature and humidity, therefore; they became fragile and brittle. Building stones in the islands are local limestone, mortars and plasters have been prepared from local sources. Halite is the dominant soluble salt detected inside building materials abreast with iron salts, while bioerosion also takes place in deterioration cycle according to the petrographic findings.

REFERENCES

Abou Ouf, M., El. Shater, A. (1992), Sedimentology and Minerology of Jizan Shelf Sediments, Red Sea, Saudi Arabia, *J.K.A.U: Mar. Sci.,* (3), pp. 39-54.

Abu-Zied, R.H., Bantan, R.A., Basaham, A.S., El Mamoney, M.H., Al-Washmi H.A. (2011), Composition, distribution, and taphonomy of nearshore benthic foraminifera of the farasan islands, southern red sea, Saudi Arabia, *Journal of Foraminiferal Research*, 41 (4), pp. 349-362.

Al Mutairi, K.A., Al-Shami, S.A., Spatial and Environmental determinants of plant diversity in Farasan Archipelago, *Saudi Arabia, Life Science Journal*, 11 (7), pp. 61-69.

Bailey, G., Al-Sharekh, A., Flemming, N., Lambeck, K., Momber, G., Sinclair, A., Vita-Finzi, C. (2007a), Coastal Prehistory in the Southern Red Sea Basin, Underwater Archaeology and the Farasan Islands, Proceedings of the Seminar for Arabian Studies (37), pp. 1-16.

Bailey, G., Flemming, N., King, G.C. P., Lambeck, K., Momber, G., Moran, L.J., Al-Sharekh, A., Vita-Finzi, C. (2007b), Coastlines, Submerged Landscapes, and Human Evolution: The Red Sea Basin and the Farasan Islands, *Journal of Island and Coastal Archaeology* (2), pp. 127-160.

Bailey, G.N., Inglis, R.H., Meredith-Williams, M., Hausmann, N., Alsharekh, A. M., Al Ghamdi, S. (2012), Preliminary report on fieldwork in the farasan islands and jizan province by the disperse project november–december, 2012, University of York, UK.

Bailey, G.N., Alsharekh, A., Flemming, N.C., Momber, G., Moran, L.J., Sinclair, A., King, G.C.P., Vita-Finzi, C., Al Ma'Mary, A., Al Shaikh, N.Y., Al Ghamdi, S. (2014), Coastal archaeology and prehistory in the Southwest Region of Saudi Arabia and the Farasan Islands: Report on the 2004 and 2006 surveys of the joint Saudi-UK Southern Red Sea Project, Coastal Prehistory in Southwest Arabia and the Farasan Islands: 2004–2009 Field Investigations, pp. 15-74.

Bantan, R.A. (1999), *Geology and Sedimentary Environments of Farasan Bank (Saudi Arabia), Southern Red Sea: A Combined Remote Sensing and Field Study*, Ph. D., Thesis, Department of Geology, Royal Holloway, University of London.

Charola, A.E., Centeno, S.A. (2002), Analysis of Gypsum-Containing Lime Mortars: Possible Errors due to the Use of Different Drying Conditions, *Journal of American Institute of Conservation* (41), pp.269-278.

Charola, A.E. (2003), Salt Deterioration: Open Questions, in Mauersalze und Architekturoberflachen (Salts in Walls and Architectural Surfaces). (Leitner, H., Laue, S., Siedel, H., Eds), Hochschule für Bildende Kunste, Dresden, pp. 10-24.

Charola, A.E., Puhringer, J., Steiger, M. (2007), Gypsum: a Review of its Role in the Deterioration of Building Materials, *Journal of Environmental Geology* (52), pp. 339-352.

English Heritage Directory of Building Limes (2000), Chapter 1 "Classification of Building Limes and Related Products", London.

JCPDS, (1967), Jaint Committee on Powder Diffraction Standards, index to the powder diffraction file, American Society for Testing and Materials, Pennsylvania, USA.

Lime-Treated Soil Construction Manual (2004), Lime Stabilization & lime modification, Published by National Lime Association "Lime", Bulletin 326.

Palomo, A., Blanco-Varela, M.T., Martinez-Ramirez, S., Puertas, F., Fortes, C. (2004), *Historic Mortars: Characterization and Durability,* New Tendencies for Research, Madrid, Spain.

Pecchioni, E., Fratini, F., Cantisani, E. (2006), The ancient mortars, an attestation of the material culture: the case of Florence, *Periodico di Mineralogia* 75 (2-3), pp. 255−262.

Reedy, Ch. L. (1994), Thin-section petrography in studies of cultural materials, *Journal of the American Institute of Conservation,* 33 (2/4), pp. 115-129.

Wüst, R.A.J., Schlüchter, Ch. (2000), The Origin of Soluble Salts in Rocks of the Thebes Mountains, Egypt: The Damage Potential to Ancient Egyptian Wall Art, *Journal of Archaeological Science* (27), pp. 1161-1172.